Amino Acids (2012) 43:483–491
DOI 10.1007/s00726-011-1105-x

ORIGINAL ARTICLE

Role of conserved active site tryptophan-101 in functional activity and stability of phosphoserine aminotransferase from an enteric human parasite

Vibhor Mishra · Ashutosh Kumar · Vahab Ali · Tomoyoshi Nozaki · Kam Y. J. Zhang · Vinod Bhakuni

Received: 4 May 2011 / Accepted: 23 September 2011 / Published online: 29 October 2011
© Springer-Verlag 2011

Abstract Site-directed mutagenesis study was performed to elucidate the role of conserved tryptophan-101 present at the active site of phosphoserine aminotransferase from an enteric human parasite *Entamoeba histolytica*. Fluorescence resonance energy transfer and molecular dynamic simulation show that the indole ring of Trp101 stacks with the cofactor PLP. Loss of enzymatic activity and PLP polarization values suggest that Trp101 plays a major role in maintaining a defined PLP microenvironment essentially required for optimal enzymatic activity. Studies on W101F, W101H and W101A mutants show that only the indole ring of the conserved Trp101 forms most favorable stacking interaction with the pyridine ring of the cofactor PLP. Protein stability was compromised on substitution of Trp101 with Phe/His/Ala amino acids. A difference in conformational free energy of 1.65 kcal mol^{-1} was observed between WT-protein and W101A mutant.

Keywords EhPSAT · Entamoeba · Site-directed mutagenesis · FRET · MD simulation

V. Bhakuni: deceased on 15th July 2011.

Electronic supplementary material The online version of this article (doi:10.1007/s00726-011-1105-x) contains supplementary material, which is available to authorized users.

V. Mishra (✉) · V. Bhakuni
Division of Molecular and Structural Biology,
CSIR-Central Drug Research Institute,
Lucknow 226001, India
e-mail: vibhor6strings@rediffmail.com;
mishravibhor@gmail.com

A. Kumar · K. Y. J. Zhang
Zhang Initiative Research Unit, Advanced Science Institute,
RIKEN, 2-1 Hirosawa, Wako, Saitama 351-0198, Japan

V. Ali
Department of Biochemistry, Rajendra Memorial Research
Institute of Medical Sciences, Agam Kuan, Patna 800007, India

T. Nozaki
Department of Parasitology, National Institute of Infectious
Diseases, 1-23-1 Toyama, Shinjuku-Ku, Tokyo 162-8640, Japan

Introduction

Functional activity of an enzyme is by virtue of certain specific amino acid residues, present in a defined active site microenvironment. Usually such residues are highly conserved for a particular enzyme as they play a specific role in enzyme catalysis. Cofactors such as pyridoxal-5′-phosphate (PLP) are additional moieties associated with enzymes which are essential for optimal enzymatic activity. Phosphoserine aminotransferase (PSAT) is one such PLP-dependent enzyme which catalyzes reversible conversion of 3-phosphohydroxy pyruvate to L-phosphoserine (Hester et al. 1999; Mishra et al. 2010). The aldehyde group of PLP is covalently linked to a conserved lysine residue at the active site (the internal aldimine). Additionally, PLP non-covalently interacts with other active site residues and such interactions are nearly conserved in PSAT (Hester et al. 1999). Our recent studies show that structural, functional and stability features of *E. histolytica* phosphoserine aminotransferase (EhPSAT) are significantly influenced by the cofactor PLP (Mishra et al. 2011).

A tryptophan residue present at the active site is strictly conserved in all PSATs. Crystallographic studies on *Bacillus alcalophilus* and *E. coli* PSAT show that this tryptophan is closely associated with the PLP (Dubnovitsky et al. 2005; Hester et al. 1999). To understand the role of the conserved active site tryptophan in functional activity

and stability of EhPSAT, a comparative site-directed mutagenesis study was performed with wild-type (WT) protein and W101A mutant. Furthermore, role of different aromatic rings in forming stacking interaction with the pyridine ring of the PLP was analyzed by a comparative study of WT-protein, W101F and W101H mutants. To the best of our knowledge this is a first attempt to understand the mode of interaction between PLP and the conserved active site tryptophan and its effect on structural/functional features of PSAT.

Materials and methods

Materials

All chemicals used in the study were purchased from Sigma-Aldrich Chemical Company; St Louis, MO.

Methods

Over-expression and purification of EhPSAT

The over-expression and purification of recombinant EhPSAT was carried out as described earlier (Mishra et al. 2010).

Cloning, over-expression and purification of W101A, W101F and W101H mutants

The W101A, W101F and W101H mutants of EhPSAT was generated using the GeneTailor™ site-directed mutagenesis system (Invitrogen) from EhPSAT gene harbored in a pET23a (+) vector (Novagen) between *Nhe*I and *Hin*dIII restriction sites. PCR was performed with primers (forward-5′-CATGTTATCTTGATACAGGAGTAGCAGCAAGTAAAGCAATAAAA-3′; 5′-GCATGTTATCTTGATACAGGAGTATTCGCAAGTAAAGCAATAAAA-3′; 5′-GCATGTTATCTTGATACAGGAGTACACGCAAGTAAAGCAATAAAA-3′ and reverse-5′-TGCTTTACTTGCTGCTACTCCTGTATCTAGATAACATGCCTTCTTATT-3′; 5′-TTCTTTTATTGCTTTACTTGCGAATACTCCTGTATCAAGATAACT-3′; 5′-TTCTTTTATTGCTTTACTTGCGTGTACTCCTGTATCAAGATAACT-3′) for the W101A, W101F and W101H mutants, respectively. PCR conditions used were: 1× 94°C for 5 min, 30× 94°C for 45 s, 54.5°C for 45 s and 72°C for 3 min and finally 1× 72°C for 10 min. The resultant constructs were sequenced to confirm the point mutation at 101 amino acid position of EhPSAT.

The resultant plasmids were transformed into *E. coli* C41 competent cells for expression. A single bacterial colony was inoculated into 5 mL of LB broth (HI media) having ampicillin at a concentration of 100 μg/mL and was allowed to grow overnight at 37°C. It was then sub-cultured in a 500 mL LB broth at 37°C until A_{600nm} of 0.6 was achieved. The culture was then induced with 0.5 mM of isopropyl-1-thio-β-D-galactopyranoside and was further incubated at 37°C for 5 h. Cells were harvested at 8,000 rpm for 10 min and the resultant pellet was suspended in 50 mM potassium phosphate (pH 8) buffer containing 300 mM NaCl, 2 mM PMSF and 10% glycerol and were disrupted using a probe type sonicator and centrifuged at 13,500 rpm for 30 min. The supernatant was applied on nickel nitrilotriacetic acid (Ni–NTA) agarose affinity column pre-equilibrated with 50 mM potassium phosphate (pH 8) buffer along with 300 mM NaCl. The column was subsequently washed with two column volumes of the same buffer and one column volume of the same buffer with 5 mM imidazole. The protein was eluted using 500 mM imidazole in the same buffer. The eluted fraction was extensively dialysed in 50 mM phosphate buffer pH 7.5 and was further loaded on a DEAE-Sepharose column which was pre-equilibrated with the same buffer. The column was washed with 2 column volumes of 50 mM phosphate buffer (pH 7.5) and with one column volume each of 25 and 50 mM NaCl in the same buffer, respectively. Finally the purified protein was eluted with 250 mM NaCl. The protein was extensively dialyzed with 50 mM phosphate buffer (pH 8) to remove the excess salt. The eluted protein was tested for purity by SDS-PAGE and ESI-MS and was found to be about 95% pure.

Spectroscopy

Fluorescence spectra were recorded on Perkin Elmer LS50b luminescence spectrometer at 25°C. Tryptophan was specifically excited at a wavelength of 295 nm and fluorescence emission was scanned between 300 and 475 nm. Fluorescence polarization for the reduced cofactor was measured at a fixed wavelength of 386 nm, and the excitation wavelength was fixed at 335 nm. 6 μM concentrations of the WT-protein and mutants were used for the experiments.

Circular dichroism (CD) experiments were performed with JASCO J810 spectropolarimeter in a 0.2 cm cell at 25°C. The far-UV CD spectra were measured at an enzyme concentration of 3 μM. Readings obtained were normalized by subtracting the baseline observed for the buffer.

Enzyme activity

The activity of the WT and mutant proteins was assessed in assay buffer containing 50 mM potassium phosphate buffer pH 8.0, 0.1 mM NADH, 32 mM ammonium acetate, 20 μM PLP, 2.0 mM glutamate, 0.35 mM phosphohydroxy pyruvate (PHP), 1 U glutamate dehydrogenase (GDH). The decrease in NADH concentration was monitored at 340 nm on a Shimadzu UV 1650PC spectrophotometer at 25°C.

GdnHCl denaturation

3 μM proteins (WT or mutants) was dissolved in potassium phosphate buffer (50 mM, pH 8.0) in the presence of increasing concentration of GdnHCl and incubated overnight at 25°C before measurements were made. Under all conditions studied overnight incubation time at different denaturant concentrations was sufficient for the reaction to achieve equilibrium.

Amino acid comparison

The amino acid sequences of phosphoserine aminotransferase from various organisms, viz. *Homo sapiens* (GI: 5326802), *Dictyostelium discoideum* (GI: 66826141), *Saccharomyces cerevisiae* (GI:640053), *Bacteroides thetaiotaomicron* (GI: 29338459), *Mus musculus* (GI:54292132), *Pseudomonas syringae* (GI:3203275481), *Yersinia pestis* (GI:115347148), *Bacillus circulans* var. *alkalophilus* (GI:51476962), *Escherichia coli* (GI:3891552) and *Entamoeba histolytica* (GI:67480029) were aligned using ClustalW software (Thompson et al. 1994).

Homology modeling, molecular dynamic simulation and computational mutagenesis

A three-dimensional model of EhPSAT was built based on four PSAT crystal structure templates *Escherichia coli*, Protein Data bank code 1BJN; *Campylobacter jejuni*, PDB code 3M5U; *Bacillus circulans* var. *alkalophilus*, PDB code 1BT4; and *Homo sapiens*, PDB code 3E77 using Modeller program (Sali and Blundell 1993). Dimer structure of EhPSAT was prepared by superimposing on their corresponding template dimers. Subsequently, a 10 ns molecular dynamics (MD) simulation was carried out for EhPSAT dimer. The protein was immersed in the rectangular truncated octahedron filled with 12 Å TIP3P water molecules and the system was then neutralized by adding Cl^- ions. The system was minimized by 500 steps of steepest descent followed by 2,000 steps of conjugate gradient. After the minimization, the system was gradually heated in the canonical ensemble from 0 to 300 K over 50 ps and additional MD simulation was performed for 500 ps for equilibration. Finally, a 10 ns MD simulation was performed under a constant temperature of 300 K. Partical Mesh Ewald (PME) was employed to deal with the long-range electrostatic interactions (Tom Darden and Pedersen 1993). The SHAKE procedure was employed to constrain all hydrogen atoms (Ryckaert and Berendsen 1977) and the time step was set to 2 fs. Trajectory snapshots were taken at every single picosecond, which were finally used for analysis. Simulations were performed on the SANDER module of Amber10 (Case et al. 2005) with amber force field (ff03). Analysis was performed using Ptraj module of Amber tools (Case et al. 2005).

W101A, W101F and W101H mutants were generated using mutagenesis utility of Pymol (The PyMOL Molecular Graphics System). The modified parameter files were generated again by using LEap module of Amber (Case et al. 2005). Subsequently, 10 ns MD simulations were carried out individually for all the three mutants to examine the effect of mutation on PLP binding affinity. Similar protocol, as described above was used for MD simulation of mutant systems.

The molecular mechanics Poisson–Boltzmann surface area (MMPBSA) implemented in Amber were used to calculate the binding free energy. The relative binding free energy was calculated as free energy difference between the WT-protein and mutants.

Calculation of free energy of stabilization

Assuming a two-state model of denaturation of the protein, the spectroscopic data were converted into the free energy (ΔG) of unfolding for each data point. For any of the points in the denaturation curve, the folded and unfolded conformations are present at significant concentration represented by:

$$f_F + f_U = 1 \quad (1)$$

f_F and f_U is the fraction of the protein present in the folded and unfolded conformations, respectively. Thus the observed value of y at any point will be

$$y = y_F f_F + y_U f_U \quad (2)$$

where, y_F and y_U represent the values of y characteristic of the folded and unfolded states, respectively, under the conditions where y is being measured. Combining Eqs. 1 and 2

$$f_U = (y_F - y)/(y_F - y_U) \quad (3)$$

The equilibrium constant, K can be calculated using Eq. 3

$$K = f_U/f_F = f_U/(1 - f_U) = (y_F - y)/(y - y_U) \quad (4)$$

The free energy change ΔG can be calculated using:

$$\Delta G = -RT \ln K = -RT \ln[(y_F - y)/(y - y_U)] \quad (5)$$

where R is the gas constant (1.987 cal mol^{-1} K^{-1}) and T is the absolute temperature (300 K). The ΔG values were then plotted against GdnHCl concentration and conformational stability in the absence of denaturant ΔG_{H20} was estimated by linear extrapolation to zero denaturant concentration.

Results and discussion

PSAT has a conserved tryptophan present at the active site

Multiple sequence alignment of PSAT from ten different origins show the presence of a conserved tryptophan residue (Fig. 1). The crystal structures of *Bacillus alcalophilus* and *E. coli* PSATs also suggest that this conserved Trp residue is present at the active site of the protein. Each subunit of the EhPSAT possesses three Trp residues, Trp32, Trp47 and the conserved Trp101 (Supplementary Fig. 1).

The cofactor PLP stacks with Trp101

EhPSAT exists as a homodimer and each subunit of the protein is composed of two domains, a large PLP-binding domain and a C-terminal domain (Fig. 2a). The enzyme harbors two active sites present at the subunit interface. The active site pocket is constituted by residues from both the PLP-binding domains of the two subunits and C-terminal domain of one subunit. All active-site residues are conserved for EhPSAT (Mishra et al. 2010, 2011). The cofactor PLP is bound by an aldimine linkage to Lys191. Additionally, PLP interacts with several other active site residues. These interactions ensure a defined PLP microenvironment which is essential for optimal enzymatic activity. The energy-minimized average simulated model of EhPSAT shows that the indole ring of Trp101 stacks with the pyridine ring of PLP at the active site and distance between the two moieties is $\sim$5 Å (Fig. 2a, inset). This stacking interaction between the PLP and Trp101 was studied by analyzing the results obtained from 10 ns MD simulation of EhPSAT. Furthermore, to elucidate the role of Trp101 in PLP binding at energetic and atomic levels, in silico mutagenesis was performed by mutating Trp101 with alanine, phenylalanine and histidine and effect of Trp101 mutation on PLP binding was again analyzed by 10 ns MD simulation for each mutant. In order to study the global conformational changes upon mutation of Trp101, we first monitored the root mean square deviation (RMSD) of backbone atoms (N, Cα, C and O) of the WT-protein and mutants (W101A, W101F and W101H) throughout the production phase trajectory from their initial configuration. Figure 2b shows the time evolution of backbone atoms of WT-protein and the mutants throughout the molecular dynamics trajectory. The RMSD versus time plots indicated that the RMSD rose initially from 1 to 3 Å for initial 5 ns after which RMSD converge to a lower value in wild-type and mutant proteins indicating that system is stabilized and there is very little global conformational change upon the mutation of Trp101 to alanine, phenylalanine and histidine. Thus, the overall structure is maintained throughout the simulation in both the WT-protein and mutants trajectories. However, an average minimum root mean square fluctuation (RMSF) per residue was observed for the WT-protein as compared to W101A, W101F and W101H mutants (Fig. 3a). The fluctuations in the per residue scan clearly suggest that the stacking interaction for W101F and W101H mutants are not as prominent as for the WT-protein. In W101A mutant, however, there are no big fluctuations but the stacking interaction is lost due to side chain truncation. Thus, the indole ring of tryptophan provides important stabilizing interactions with pyridine ring of PLP, attenuating the movement of PLP within active site.

To further examine the behavior of stacking between indole ring of Trp101 and pyridine ring of the PLP and effect of different side chains of Phe/His/Ala mutants on this stacking interaction, the distance between the centroid of indole ring of Trp101 for WT-protein, Cβ of alanine for W101A mutant, centroid of phenyl ring of phenyl alanine for W101F mutant and centroid of imidazole ring of histidine for W101H mutant with centroid of pyridine ring of PLP was calculated throughout the molecular dynamics trajectory. The time evolution of this stacking interaction is shown by distance plot where the stacking interaction between pyridine ring of PLP and indole ring of Trp101 is maintained at a distance of $\sim$5–6 Å and has low deviations throughout the trajectory (Fig. 3b). The average distance between pyridine ring of PLP and indole

```
Human          TENLVRELLAVPDNYKVIFLQGGGCGQFSAVPLNLIGLKA-----GRCADYVVTGAWSAK 110
Mouse          TENLVRELLAVPNNYKVIFVQGGGSGQFSAVPLNLIGLKA-----GRSADYVVTGAWSAK 110
Dictyostelium  TKSNLKKLLSISDDYDILFLQGGASSLFAGIPMNLCENGV-----EDIVDFIVTGSWSKQ 113
Entamoeba      TKALMKEVMDIPEGYEILFFGGGASLQFLMVAMNLLN---------KKACYLDTGVWASK 104
Bacteroides    AEALFKELLNIPEGYSVLFLGGGASMEFCMVPFNFLE---------KKAAYLNTGVWAKK 102
Bacillus       AQARLLALLGNPTGYKVLFIQGGASTQFAMIPMNFLKE-------GQTANYVMTGSWASK 106
Escherichia    AEKDFRDLLNVPSNYKVLFCHGGGRGQFAAVPLNILGD-------KTTADYVDAGYWAAS 103
Yersinia       SEKDLRDLLQIPANYKVLFCHGGARAQFAAVPLNLLGD-------RNSADYIDGGYWAHS 105
Pseudomonas    AEQDLRDLLSIPSNYKVLFLQGGASQQFTQIALNLLPE-------NGKADYIDTGIWSQK 106
Saccharomyces  SKKHLIELLNIPDTHEVFYLQGGGTTGFSSVATNLAAAYVGKHGKIAPAGYLVTGSWSQK 116
```

Fig. 1 Amino acid sequence alignment of PSAT from various sources. The conserved tryptophan residue is *highlighted*

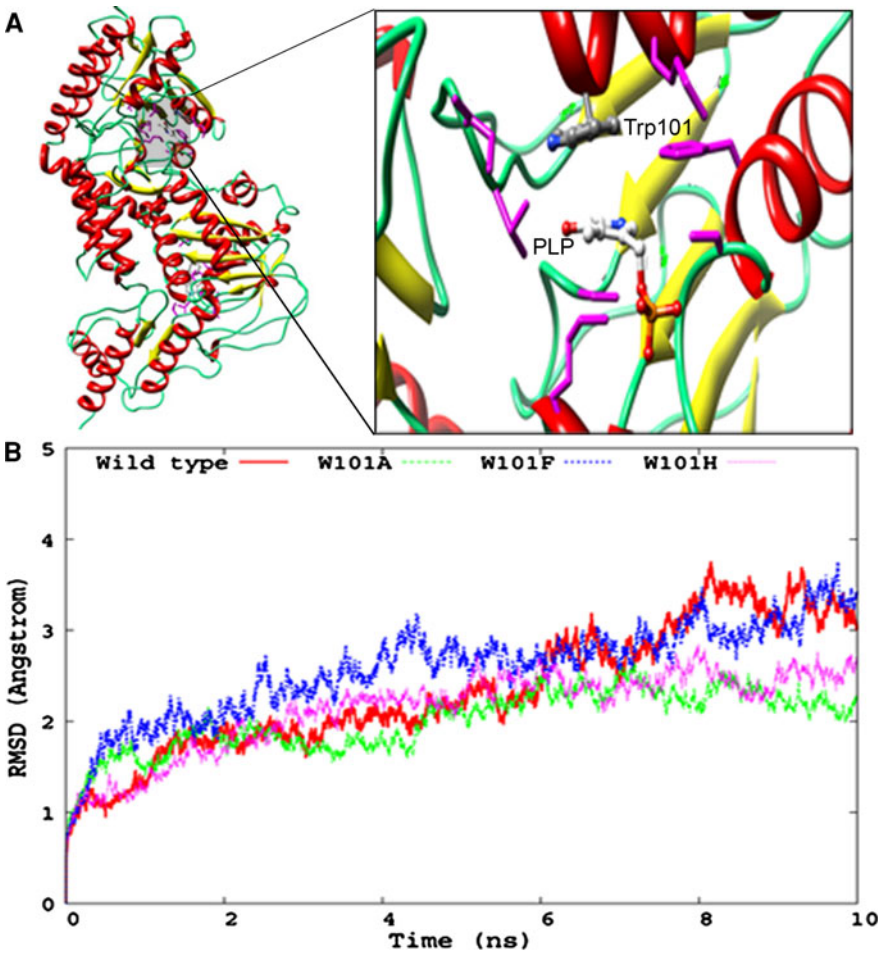

Fig. 2 **a** Energy minimized average simulated model EhPSAT. α- helices, β- sheets and random coils are shown in *red*, *yellow* and *green* colors, respectively. *Inset*, a magnified snapshot of the active site showing the cofactor PLP stacked with Trp101. **b** A root mean square deviation (RMSD) versus time plot along the molecular dynamic simulation trajectory of WT-protein (*red*, *solid line*), W101A (*green*, *dashed line*), W101F (*blue*, *dotted line*) and W101H (*purple*, *dash-dotted line*) mutants (color figure online)

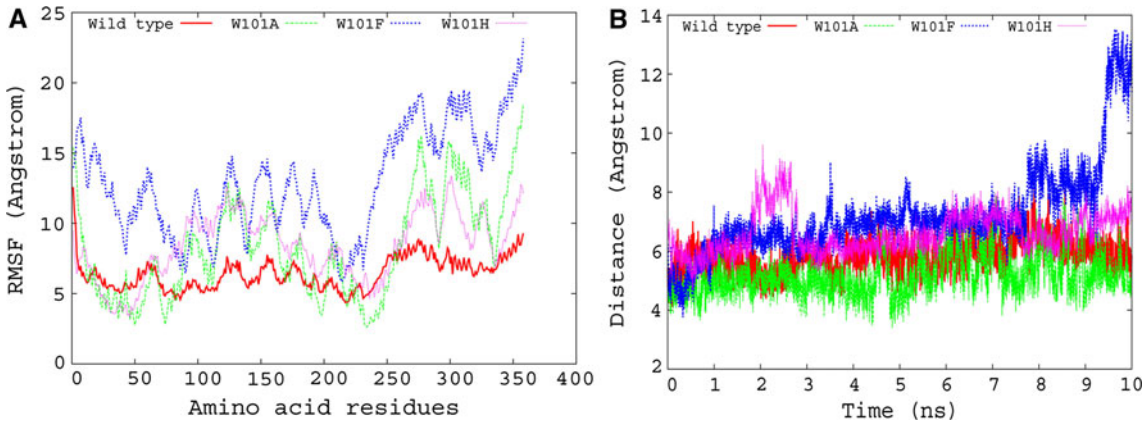

Fig. 3 **a** A plot of root mean square fluctuations (*RMSF*) per residue of WT-protein (*red*, *solid line*), W101A (*green*, *dashed line*), W101F (*blue*, *dotted line*) and W101H (*purple*, *dash-dotted line*) mutant proteins. **b** A distance plot along the simulation trajectory between the centroid of the indole ring of tryptophan in the WT-protein (*red*, *solid line*), Cβ of alanine for W101A mutant (*green*, *dashed line*), centroid of benzene ring of phenyl alanine for W101F mutant (*blue*, *dotted line*) and centroid of imidazole ring of histidine for W101H mutant (*purple*, *dash-dotted line*) with centroid of pyridine ring of PLP

ring of Trp101 (WT-protein), Ala101 (W101A), Phe101 (W101F) and His101 (W101H) mutants is 5.81, 5.14, 7.22 and 6.62 Å, respectively. Fluctuations were observed for W101F and W101H mutants in the respective distance between the amino acid side chains of Phe/His and PLP throughout the MD simulation trajectory (Fig. 3b). Thus,

the results suggest that only the indole ring of Trp101 maintains optimum proximity with pyridine ring of PLP which is essential for stacking of the two moieties.

Fluorescence resonance energy transfer (FRET)

EhPSAT shows FRET between the PLP and Trp101, suggesting that the two fluorophores are closely associated with each other (Mishra et al. 2010). However, fluorescence scan of W101A mutant showed no FRET as the aromatic side chain of Trp101 is absent in this case (Fig. 4). The other two tryptophan residues, i.e., Trp32 and Trp47 are not close enough to the PLP to support efficient energy transfer between the two fluorophores (Supplementary Fig. 1). The average distance calculated between centroid of pyridine ring of PLP and indole ring of Trp32, Trp47 and Trp101 is 33.64, 26.84 and 5.81 Å, respectively, along the MD simulation trajectory (Supplementary Fig. 2). Since an average distance of ~5–10 Å is essential for transferring energy of excited electrons from one fluorophore (donor) to another fluorophore (acceptor), we observed FRET only between Trp101 and PLP for the WT-protein (Cai and Schirch 1996; Chaturvedi and Bhakuni 2003; Lakowicz 2006; Mishra et al. 2010). The other two tryptophans, i.e., Trp32 and Trp47 are distantly located from the cofactor PLP which resulted in absence of FRET in W101A mutant. In case of W101H and W101F also FRET was not observed (data not shown). Furthermore, the absence of FRET for W101F mutant is because the emission wavelength of phenyl alanine (285 nm) does not overlap with the excitation wavelength of PLP (335–340 nm). Histidine in itself is not an intrinsic fluorophore and thus no FRET was observed in the case of W101H mutant.

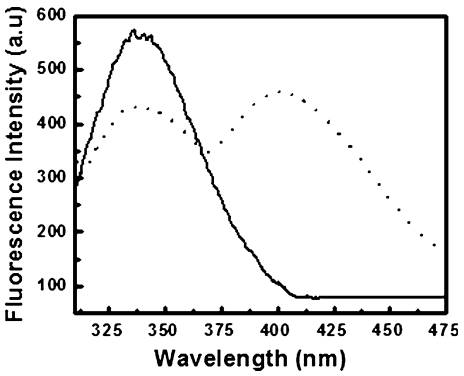

Fig. 4 Fluorescence resonance energy transfer WT-protein (*dashed line*) and W101A mutant (*solid line*)

Enzymatic activity

Site-directed mutagenesis is a perfect tool to identify the important active site residues and to analyze their specific role in enzyme catalysis. The enzymatic activity of EhPSAT was significantly perturbed by substitution of active site Trp101 residue, as the W101A mutant showed a residual activity of about 5% as compared to the WT-protein (Fig. 5a). The results suggest that Trp101 is essential for the optimal activity of the enzyme. Since Trp101 stacks with the cofactor (as discussed above) changes in the PLP microenvironment because of the W101A mutation might explain the observed loss in the enzymatic activity. Furthermore, W101F and W101H mutants were used to analyze the effect of other aromatic rings on the functional activity of EhPSAT. W101H and W101F mutants showed 20 and 70% activities, respectively, as compared to the WT-protein. Histidine has an imidazole ring as a side chain which does not provide sufficient stacking with the cofactor PLP. This may be a strong reason for low enzymatic activity of the W101H mutant. However, as compared to alanine ($-CH_3$ side chain) imidazole very poorly stacks with the cofactor PLP which results in slight increase in the residual activity of W101H mutant as compared to W101A mutant. Phenyl alanine, on the other hand has a benzene ring present as a side chain which efficiently stacks with the pyridine ring of the PLP when compared with the histidine or alanine side chains of the W101H or W101A mutants and that results in an increased residual activity of 65–70%. The results clearly suggest that the side chain of tryptophan residue is best suited for favorable interactions with the cofactor PLP. None of the mutants showed enzymatic activity equivalent to the WT-protein. This further explains that during the course of evolution tryptophan is been selected over the other amino acid residues for PSAT as an efficient stacking partner for the cofactor PLP.

Fluorescence polarization

Subtle changes in the cofactor microenvironment can significantly perturb the enzymatic activity. Hence, it was important to analyze the changes in the PLP microenvironment of EhPSAT by studying dynamics of the protein-bound cofactor. Studies on various PLP-dependent proteins show that the prosthetic group PLP exhibits different spectral characteristics in different proteins, reflecting specific environmental property of the cofactor (Mishra et al. 2010). For this reason PLP has been used as a natural marker to probe dynamic microenvironment of the cofactor in proteins (Mishra et al. 2010). Figure 5b shows the changes in PLP fluorescence polarization for WT-protein, W101F, W101H and W101A mutants. The polarization

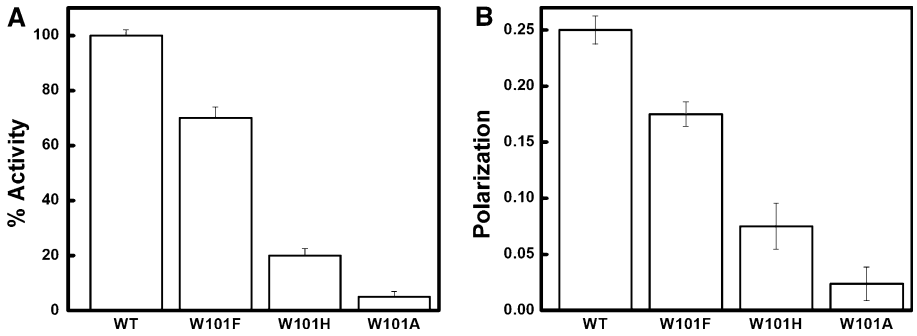

Fig. 5 **a** Bar diagram showing the enzymatic activity of WT-protein, W101F, W101H and W101A mutants. **b** Bar diagram showing cofactor polarization values of WT-protein, W101F, W101H and W101A mutants

values observed for the mutants were significantly reduced as compared to the WT-protein suggesting that Trp101 specifically modulates the flexibility of the protein-bound cofactor PLP. Furthermore, polarization values for W101F, W101H and W101A mutants followed a descending trend, respectively. The results suggest that the benzene ring of phenyl alanine (W101F) moderately stacks with the pyridine ring of PLP, the imidazole ring of histidine (W101H) stacks poorly with the cofactor and finally the $-CH_3$ side chain of alanine (W101A) shows almost no stacking interaction with the PLP. Highest polarization values for the WT-protein shows that the side chain of the tryptophan residues stacks most efficiently with the pyridine ring of the cofactor PLP and helps in modulating the orientation of the cofactor in the active site. To further elucidate the role of Trp101 in PLP binding, MM-PBSA approach was used to calculate the binding free energy calculation for WT-protein, W101A mutant. The binding energy difference was calculated according to the following equation:

$$\Delta\Delta G = \Delta G_{\text{wildtype}} - \Delta G_{\text{mutant}}. \quad (6)$$

According to MM-PBSA binding free energy calculations, the PLP binding affinity is decreased by 1.96 kcal/mol when Trp101 is mutated with alanine. This suggests that Trp101 is important for the binding of PLP in a specific orientation to the active site of EhPSAT. The results also suggest that van der Waals interactions are primarily involved in favorable contributions to binding free energy when side chain ring of Trp101 stacks with PLP. Mutation of Trp101 with Ala101 leads to decrease in van der Waals contribution which leads to decrease in overall binding free energy (data not shown).

Interactions which fix the position and orientation of the cofactor in the active site play a significant role in enzyme catalysis of the aminotransferases (Hester et al. 1999). This is probably because upon binding of the substrate, the lysine is exchanged for the amino group of the substrate forming a Schiff-base complex with the PLP (external aldimine). In the next step one of the bonds to the Cα atom of the external aldimine is broken resulting in the formation of a quinonoid intermediate (Hester et al. 1999). In the final step, the processed amino acid product moves out of the active site and the internal aldimine linkage is restored. The pyridine ring of PLP is a bulky group which needs to be positioned in a defined orientation to interact with the incoming substrate to form an external aldimine. Stacking interactions with a similar or look-alike (ringed) moiety would be the best suited option for achieving and maintaining such conformation. Tyrosine, phenylalanine, histidine and tryptophan are the four possible options available with the protein as only these four amino acids possess side chains which can stack with the pyridine ring of the PLP. Histidine has an imidazole ring as a side chain which makes it a weak stacking partner with the pyridine ring of the PLP. Since tyrosine has terminal -OH group which can interfere with the electrostatics of the enzyme-catalyzed reaction the other two amino acids, i.e., phenylalanine and tryptophan are best suited for the job because of their inert nature. Our survey of the amino acid sequences of PSAT from various organisms across the species clearly shows that the amino acid tryptophan is present stacked with the PLP in almost 99.5% of the cases. On very rare occasions, for example in *Mycobacterium tuberculosis* phenyl alanine is present instead of tryptophan.

Thus, a substitution of the bulky side chain of Trp101 with alanine which has methyl group ($-CH_3$) side chain causes significant changes in the PLP microenvironment which eventually results in the loss of enzymatic activity.

Protein stability

Equilibrium unfolding studies of a protein using denaturants provide a measure of its conformational stability (Mishra et al. 2011). Thus, GdnHCl-induced denaturation studies were performed to monitor alterations in the tertiary and secondary structure of the WT-protein and the mutants using tryptophan fluorescence and far UV-CD signal at 222 nm, respectively (Fig. 6a). The denaturation curves showed a superimposable sigmoidal dependence of these changes suggesting GdnHCl-induced unfolding of EhPSAT

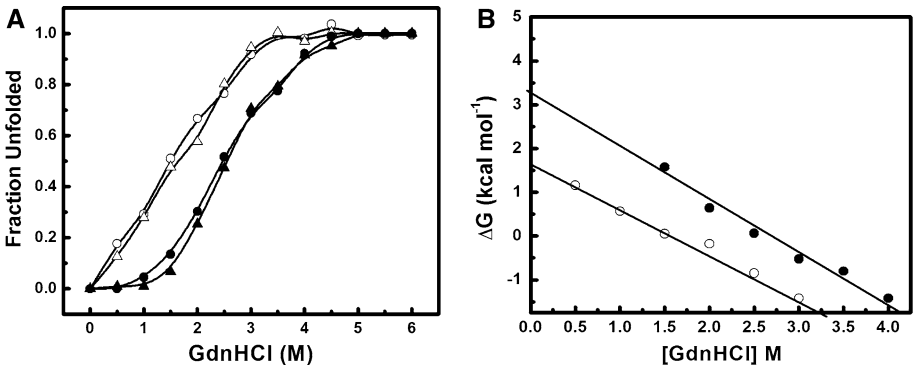

Fig. 6 **a** GdnHCl-induced denaturation of WT-protein and W101A mutant as monitored by changes in tryptophan fluorescence emission maxima for WT-protein (*filled triangle*), W101A mutant (*open triangle*) and loss of CD ellipticity at 222 nm for WT-protein (*filled circle*) and W101A mutant (*open circle*), respectively. **b** A linear free energy extrapolation curve of WT-protein (*filled circle*) and W101A mutant (*open circle*) with respect to [GdnHCl]. The ΔG_{H20} was the intercept on the *Y*-axis, obtained using the linear extrapolation

to be a two-state process. For proteins with two-state transition, the *Cm* value (denaturant concentration at which 50% denaturation process is completed) obtained from the analysis of the solvent denaturation curve intrinsically serves as a probe for its stability to the chaotrope (Akhtar et al. 2002). Interestingly, the *Cm* values obtained from the denaturation profile for WT-protein and W101A mutant were 2.75 and 1.7 M, respectively. The results show that *Cm* observed for the W101A mutant was considerably lower than for the WT-protein suggesting that the alanine mutation leads to destabilization of the protein (Fig. 6a). The *Cm* values for the W101F and W101H mutants was in between the values observed for the WT-protein and W101A mutant (data not shown). The quantitative analysis of the spectroscopic data obtained from the denaturation study allows estimation of protein stability in the absence of denaturant. The GdnHCl-induced denaturation curves of WT and W101A mutant proteins were used to determine the free energy of stabilization in the absence of denaturants (ΔG_{H20}) by linear extrapolation of the ΔG values to zero denaturant concentration (Pace 1986). From these measurements ΔG_{H20} values were calculated to be around 3.3 ± 0.12 and 1.65 ± 0.14 kcal mol^{-1} for WT-protein and W101A mutant, respectively, 25°C (Fig. 6b). The energy difference between the WT-protein and the W101A mutant, calculated according to the Eq. 6 was 1.65 kcal mol^{-1}. These observations are in close agreement with the energy difference calculated from MD simulations (discussed earlier). Thus, the results suggest that Trp101 is important for protein stability. Our recent studies show that the cofactor PLP plays a major role in stability of the protein as the apo-enzyme was thermodynamically unstable when compared with the holo-enzyme (Mishra et al. 2011). W101A mutation significantly perturbs the interactions which help in maintaining a close association of cofactor with the protein. Thus, the cofactor is loosely associated with the protein which explains the loss of thermodynamic stability of the W101A mutant.

Conclusions

Trp101 of EhPSAT is a conserved amino acid residue present at the active site of the protein. The indole ring of the Trp101 is stacked with the pyridine ring of the cofactor PLP. Substitution of Trp101 with an alanine residue imparts significant loss in the enzymatic activity. This can be attributed to amino acid side chain-driven changes in PLP microenvironment which was further studied by substituting the side chain of tryptophan with aromatic rings of phenyl alanine (W101F) and histidine (W101H) mutants. A direct correlation can be established between the flexibility of cofactor conformation and activity of the enzyme. The stability of the protein was also compromised with substitution of Trp101 with Phe/His/Ala amino acids. The study demonstrates that the conserved Trp101 present at the active site significantly influences PLP microenvironment of EhPSAT.

Acknowledgments In acknowledgement of his formidable biological insights and inspirational mentorship that guided this work VM, AK, VA, KYJZ and TN dedicate this paper to the memory of our co-author, Vinod Bhakuni. We thank Md. Sohail Akhtar for useful discussions and/or comments on the manuscript. VM is thankful to CSIR New Delhi for senior research fellowship. This is communication no. 8136 from CSIR-CDRI.

Conflict of interest None declared.

References

Akhtar MS, Ahmad A, Bhakuni V (2002) Guanidinium chloride- and urea-induced unfolding of the dimeric enzyme glucose oxidase. Biochemistry 41:3819–3827

Cai K, Schirch V (1996) Structural studies on folding intermediates of serine hydroxymethyltransferase using fluorescence resonance energy transfer. J Biol Chem 271:27311–27320

Case DA, Cheatham TE 3rd, Darden T, Gohlke H, Luo R, Merz KM Jr, Onufriev A, Simmerling C, Wang B, Woods RJ (2005) The Amber biomolecular simulation programs. J Comput Chem 26:1668–1688

Chaturvedi S, Bhakuni V (2003) Unusual structural, functional, and stability properties of serine hydroxymethyltransferase from *Mycobacterium tuberculosis*. J Biol Chem 278:40793–40805

Dubnovitsky AP, Ravelli RB, Popov AN, Papageorgiou AC (2005) Strain relief at the active site of phosphoserine aminotransferase induced by radiation damage. Protein Sci 14:1498–1507

Hester G, Stark W, Moser M, Kallen J, Markovic-Housley Z, Jansonius JN (1999) Crystal structure of phosphoserine aminotransferase from *Escherichia coli* at 2.3 Å resolution: comparison of the unligated enzyme and a complex with alpha-methyl-l-glutamate. J Mol Biol 286:829–850

Lakowicz JR (2006) Principles of fluorescence spectroscopy, 3rd edn. Springer, New York

Mishra V, Ali V, Nozaki T, Bhakuni V (2010) *Entamoeba histolytica* phosphoserine aminotransferase (EhPSAT): insights into the structure–function relationship. BMC Res Notes 3:52

Mishra V, Ali V, Nozaki T, Bhakuni V (2011) Biophysical characterization of *Entamoeba histolytica* phosphoserine aminotransferase (EhPSAT): role of cofactor and domains in stability and subunit assembly. Eur Biophys J 40:599–610

Pace CN (1986) Determination and analysis of urea and guanidine hydrochloride denaturation curves. Methods Enzymol 131:266–280

Ryckaert Jean-Paul, Berendsen HJC (1977) Numerical integration of the Cartesian equations of motion of a system with constraints: molecular dynamics of *n*-alkanes. J Comp Phy 23:321–341

Sali A, Blundell TL (1993) Comparative protein modelling by satisfaction of spatial restraints. J Mol Biol 234:779–815

Thompson JD, Higgins DG, Gibson TJ (1994) CLUSTAL W: improving the sensitivity of progressive multiple sequence alignment through sequence weighting, position-specific gap penalties and weight matrix choice. Nucleic Acids Res 22:4673–4680

Tom Darden DY, Pedersen Lee (1993) Particle mesh Ewald: an N − log(N) method for Ewald sums in large systems. J Chem Phys 98:10089–10092

The PyMOL Molecular Graphics System Vrp. Schrödinger, LLC